Bulletin of the Seismological Society of America. Vol. 68, No. 4, pp. 1013–1030, August 1978

t^* FOR S WAVES WITH A CONTINENTAL RAY PATH

BY L. J. BURDICK

ABSTRACT

The purpose of this study was to determine t^* for S waves with ray paths under the continental United States. The data set consists of long- and short-period body waves from the Borrego Mountain earthquake as observed in the northeastern U.S. The P wave forms are dominated by the sP phase and the SH wave forms by the sS. It is assumed that there are no losses in pure compression so that the relative attenuation rate of P and S waves is known. The initial source radiation is determined from the sP phase and the value of t_β^* from the spectral content of the S wave. The results indicate that t_β^* is 5.2 ± 0.7 sec along this ray path. Long- and short-period body waves from some deep South American events are used to test for lateral asymmetry of the Q distribution under the U.S. No lateral amplitude variation exists in this data, but this result is difficult to correlate with many previous results. The t_β^* value for a 600-km deep earthquake appears to be about 3 sec. A comparison of these values with values computed from current models of the Earth's Q distribution indicates that the models are slightly too high in Q overall and that more of the total body-wave attenuation occurs above 600 km than is indicated by the models.

INTRODUCTION

The attenuation rate of body waves is generally parameterized either by the average quality factor along the ray path, Q_{av}, or by the quantity t^*. This is defined as the integral over time along the ray path of inverse Q

$$t^* = \int_{\text{ray path}} \frac{dt}{Q}. \tag{1}$$

Carpenter (1967) suggested the approximate, but more convenient form for this expression

$$t^* = T/Q_{av} \tag{1a}$$

where T is the total travel time of the ray. t^* is given a subscript α for P waves or β for S waves. Since body-wave travel times are well known, the two parameterizations are interchangeable. Most previous measurements of t_α^* for teleseismic body waves have yielded values around 1 sec and those of t_β^* around 4 sec (Anderson and Hart, 1978; Marshall *et al.*, 1975). The values appear to be roughly independent of epicentral distance for $20° < \Delta < 80°$, but they do depend on source depth.

A very common method for determining Q_{av} has been to measure the attenuation of successive multiples of the ScS phase on long-period records (Kovach and Anderson, 1964; Sato and Espinoza, 1967; Yoshida and Tsujiura, 1975; Jordan and Sipkin, 1977). Other methods have involved measuring the spectral content of direct P and S waves from long-period seismometers (Solomon and Toksöz, 1970; Mikumo and Kurita, 1968; Teng, 1968). A few studies have used P waves recorded on short-period instruments (Kanamori, 1967a; Frasier and Filson, 1972) and fewer still have used short-period S waves (Marshall *et al.*, 1975; Kanamori, 1967b; Choudhury and

Dorel, 1973). Marshall *et al.* (1975) pointed out that the short-period teleseismic S waves merited much closer examination because the effect of anelastic attenuation on them is overwhelming. Since the effect can be easily discerned in the short-period S wave data, it can be reliably measured. The purpose of this report is to present some new measurements of t_β^*. They have been determined from teleseismic S waves recorded on both the WWSSN short-period and long-period instruments. The short- and long-period P waves have been used to constrain the initial source radiation in the period range spanned by the two instruments. Theoretical source models and a theoretical relationship between t_α^* and t_β^* have been used to relate the observed P waves to the observed S waves.

t^* for a Surface Focus Event

The S waves from the April 9, 1968 Borrego Mountain earthquake (Hanks and

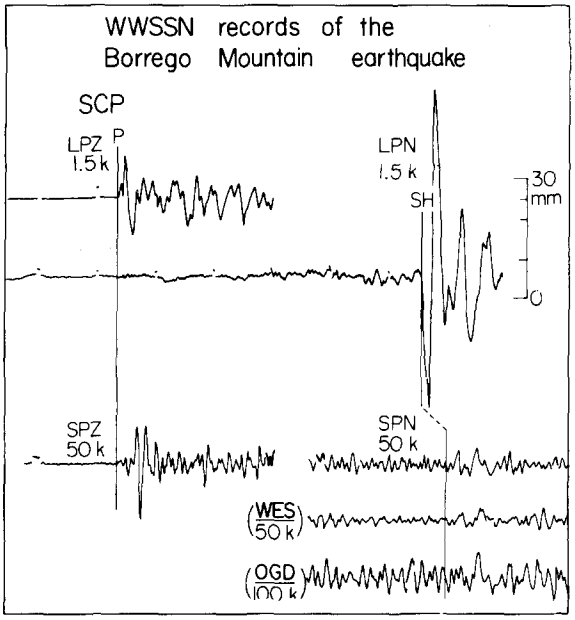

FIG. 1. The figure shows the long- and short-period records of the Borrego Mountain earthquake at SCP. The P waves are simple and clear. The long-period N component is very nearly pure SH. The short-period S waves are very small because they have been severely attenuated.

Wyss, 1972; Burdick and Mellman, 1976) recorded at WWSSN stations in the northeastern U.S. are especially well suited for determining t_β^*. The records are low noise and the stations are oriented so the NS component is nearly pure SH. The distance range is between 30° and 40°, so the effects of the velocity structure of the mantle on the direct arrivals are negligible. Most importantly, the effects of attenuation are very dramatic and can be seen easily in the records.

The Data Set. Figure 1 shows the P and SH wave forms from State College, Pennsylvania (SCP, $\Delta = 31.3°$). The long-period instruments have a gain of 1.5K. At this setting, the P wave is of moderate size. The long-period S is large but still on scale. The short-period instruments are at 50K gain, so the short-period P is slightly larger than the long-period P. However, the short-period S barely emerges from the background noise even though the long-period S is very much larger than the long-period P. This is because the short-period S energy has been attenuated much more heavily than the P.

Also shown in Figure 1 are the short-period SH records from Weston, Massachu-

setts (WES, $\Delta = 36.3°$) and Ogdensburg, New Jersey (OGD, $\Delta = 33.4°$). The short- and long-period records from these stations have also been used in this study. Like the short-period SCP S wave, the WES and OGD short-period S waves are very small. The signal-to-noise ratio at SCP and WES is about 2/1 and at OGD only about 1/1. Nonetheless, it is possible to make a meaningful measurement of t_β^* from only a rough estimate of the amplitudes of these short-period S waves.

We can be certain at the outset that the evidence for heavy attenuation of the S waves which is illustrated by Figure 1 is not a source effect. As we shall show, the

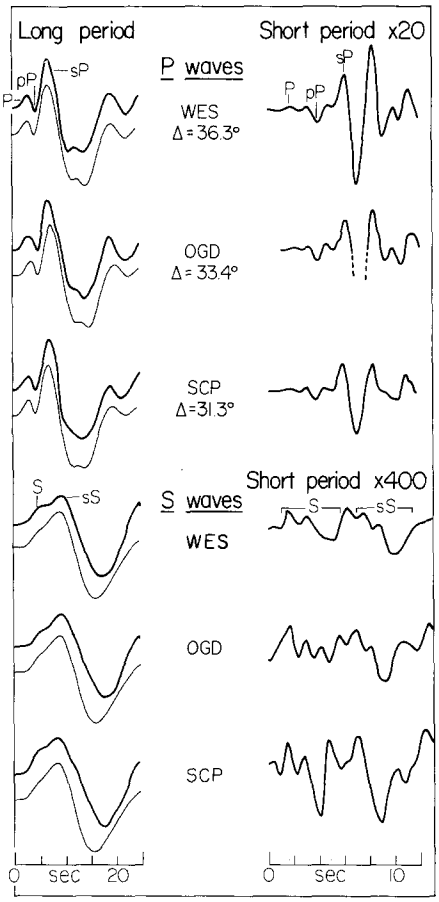

FIG. 2. The figure shows the long- and short-period records to be used in the study. All long-period records are normalized to 1. The corresponding short-period P records are magnified by a factor of 20 with respect to the long, and the short-period S records by a factor of 400. The short-period S waves are much smaller than the P because they have been more heavily attenuated.

P wave form is dominated by the sP arrival and the S wave form by the sS arrival. This means that the strongest arrivals in the P and S wave codas must have had nearly identical radiation from the source. This knowledge of the relative strengths of the surface phases illustrates the final reason for using the S waves from the Borrego Mountain event. The source has been studied extensively and a very accurate source model is available (Burdick and Mellman, 1976). This model makes it possible to separate the effects of attenuation from the effects of the source.

Figure 2 shows all of the data to be used in determining t_β^* on an expanded time scale. Synthetics for the long-period records are compared with the data to show how well the source model predicts the ground motion at these particular stations.

From the theoretical source model, we know that the P and pP appear as small precursors on the long-period P wave form. The dominant arrival is the sP phase. The three arrivals are marked on the WES record in Figure 2. The sS phase is about twice the size of the S phase. The arrivals are marked on the WES SH wave form in the figure. It is important to note that the synthetic seismograms in Figure 2 were computed for a point source. This means that the effects of fault directivity were ignored and a single source pulse was used for all phases. The study of Burdick and Mellman (1976) demonstrated that a simple point source model works well for all of the long-period Borrego Mountain wave form data and that reasonable finite fault models for the event do not predict strong directivity effects. This observation will play a key role in the ensuing arguments since it will allow us to relate the initial source pulses of the S, sS, and sP phases. In Figure 2, all of the long-period records have been normalized to unit amplitude. The S waves have been reversed in sign so that all of the records would have the same polarity. The short-period P records have been magnified 20 times and the short-period S records 400 times with respect to the corresponding long-period records. The wave forms are much less consistent because the signal-to-noise ratio is so much smaller. In Figure 2, the short-period sP and sS phases appear to be roughly the same size. Since the short-period P wave forms are magnified 20 times and the short-period S wave forms 400 times, the short-period to long-period ratio of the sS phase is at least 20 times smaller than the sP ratio. These two phases leave the seismic source with very nearly the same vertical takeoff angle. As will be demonstrated in a following section, this means that fault directivity does not cause strong differences in the frequency content of the two pulses. Yet when the waves arrived at the receiver, the short-period energy which traveled in the shear mode was attenuated much more than the short-period energy which traveled in the compressional mode. The effects of anelasticity can be easily seen in the records and reliably measured.

It may seem that it would have been preferable to use a larger source event than the Borrego Mountain earthquake in order to increase the amplitude of the short-period S waves. However, this is not the case. To take complete advantage of the WWSSN instrument system, it is also necessary to have good estimates of the long-period S amplitudes. The SCP SH record at 1.5K gain is about half the possible amplitude scale. The WES and OGD SH records are as large as they can be without going off scale. The majority of WWSSN long-period instruments are run at either 1.5 or 3.0K gain. In those instances where the long-period level is reduced, the short-period gain is generally also reduced. Therefore, if a larger earthquake were used, either the long-period records would be off scale or the short-period records would still be very small. Also, the sources of events larger than Borrego Mountain are almost always complex multiple events which are very difficult to model. All in all, the data set to be used here is as good as any which might be found for determining $t_\beta{}^*$ from direct S waves.

Data Analysis. There are two major difficulties involved in extracting the value of $t_\beta{}^*$ from the data set. The first is that the interaction of the direct phase with the surface phases plays a dominant role in determining the shapes of the long-period P and S wave forms. This can be most easily compensated for by computing time-domain synthetics rather than trying to fit Fourier spectra. The second difficulty with the data is the poor signal-to-noise ratio of the short-period S waves. A simple measurement of the maximum trace amplitude would be an unreliable indicator of the size of the wave. A more sophisticated measurement of the signal strength is required. The parameter which will be used to quantify the amplitudes of the S

records will be designated as r_s or the S-wave power ratio. It is defined as

$$r_s = \int_0^T [SP(t) \cdot W(t)]^2 \, dt / \int_0^T [LP(t) \cdot W(t)]^2 \, dt. \tag{2}$$

$SP(t)$ and $LP(t)$ are the long- and short-period records normalized to unit gain and $W(t)$ is a trapezoidal time window. T, the total length of the window, is 14 sec. The trapezoid has a 2-sec rise time, a 10-sec level time, and a 2-sec fall off time. The window is positioned so that it begins 2 sec before the estimated arrival time. In time domain, r_s is simply the ratio of the average squared amplitudes of the short- and long-period signals. In frequency domain, the reasons for choosing this particular amplitude measure are more apparent. From Parseval's theorem, we know that the quantity in the numerator of equation (2) is just the power in the frequency band of the short-period instrument, providing that $W(t)$ is much longer than the instrument response time. The quantity in the denominator is the power in the lower frequency band of the long-period instrument. The time window is long enough so that it will not have a strong effect. The quantity r_s is then the ratio of the power in the two frequency bands defined by the two WWSSN instruments. It is a rough but stable estimate of the spectral content of the wave which uses the natural characteristics of the WWSSN recording package to best advantage. r_s depends only on the spectrum of the ground motion. All scaling effects such as the source moment and geometric spreading are divided out by taking the short- to long-period power ratio. The values of r_s measured from the three SH records shown in Figure 2 were $(0.23 \pm 0.07) \times 10^{-5}$ for WES, $(0.25 \pm 0.14) \times 10^{-5}$ for OGD, and $(0.38 \pm 0.17) \times 10^{-5}$ for SCP. The error estimates are just the average power in an equivalent segment of background noise. They were found by measuring the power in the 60 sec of leakover P coda immediately preceeding the SH wave and adjusting for the shorter window actually used on the data.

Calculated Values of r_s. Theoretical values for S-wave power ratio can be calculated by computing long- and short-period seismograms and processing them in the same way as the data. Since both the data and the synthetics are processed in exactly the same way the measurements of r_s from each should be directly comparable. If the theoretical wave forms are computed for a range of t_β*'s, a smooth curve can be generated in the $t_\beta^* - r_s$ plane. The intersection of this curve with the observed levels of r_s should give the t_β^* value for North America. Unfortunately, there is a major ambiguity still to be dealt with. The value of r_s will depend critically on the initial source spectra of the S and sS phases as well as on t_β^*. It is necessary to obtain accurate estimates of the original shapes of these pulses. As was pointed out previously, the assumption that all phases radiated by the source had identical frequency content worked very well in the long-period wave form modeling study. Therefore, the approach which will be used here will begin with a determination of the pulse shape of the sP phase from the P-wave records. This will be accomplished by using a simultaneous long period-short period deconvolution technique. The synthetic SH waves will then be calculated by using the deconvolved sP pulse as a model for the S and sS pulses. In a separate calculation, some theoretical fault models will be considered to test the validity of this technique. The procedure for simultaneously deconvolving the attenuation corrected instrument responses from the short- and long-period P records was outlined in Burdick (1977). The result from Burdick and Mellman (1976) for the WES record from the Borrego Mountain

earthquake is illustrated in Figure 3. In order to correct the instruments for attenuation, it is necessary to know the value of t_α^*. A relationship exists between t_α^* and t_β^* which effectively reduces the problem back to a single unknown. Anderson *et al.* (1965) showed that if there are no losses in pure compression

$$\frac{Q_\beta}{Q_\alpha} = \frac{4}{3}\frac{\beta^2}{\alpha^2} \tag{3}$$

where β and α are the elastic-wave velocities. The results of both that study and the more recent study of Anderson and Hart (1977) indicate that the compressional

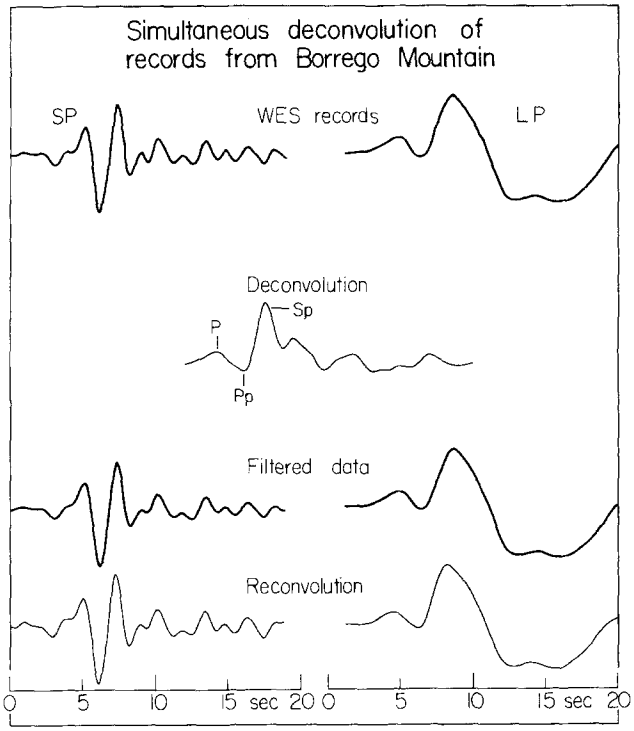

FIG. 3. The deconvolution result which is shown in the second row is a time function which is compatible with both the long- and short-period records of the Borrego Mountain earthquake. It was obtained by simultaneously deconvolving the top two traces [see equation (6a)]. The third row shows the data filtered by the deconvolution filter. The bottom traces are the result of reconvolving the deconvolution result with the instruments. If the deconvolution result is sufficiently stable, the bottom two rows should be the same.

losses in the Earth are negligible, so that equation (3) is approximately true. The lack of attenuation of pure compressional motion merely indicates that shear mechanisms such as grain boundary sliding dominate the attenuation process. In the 30° to 80° range, the P and S waves have very similar ray paths. If it is assumed that $\lambda \approx \mu$ along the path then

$$Q_\alpha = \frac{9}{4} Q_\beta. \tag{4}$$

The ratio of the travel times of the direct P and S waves at 33° is $T_\beta/T_\alpha = 1.80$. Combining these results gives the familiar expression

$$t_\beta^* = 4\, t_\alpha^*. \tag{5}$$

If a value of $t_\alpha{}^*$ is assumed, a corresponding estimate of the sP pulse can be obtained by deconvolution. The synthetic SH wave forms are then computed using the sP pulse as the source pulse and the $t_\beta{}^*$ dictated by equation (5). The expression for the synthetic seismogram $S(t)$ is

$$S(t) = I(t) * A(t, t^*) * P(t) \tag{6}$$

I is the appropriate instrument response, * is the convolution operator, $A(t, t^*)$ is the Futterman (1962) attenuation operator, and $P(t)$ is the source pulse. The source pulse includes the interaction of the basic pulse shape with the free surface. It is

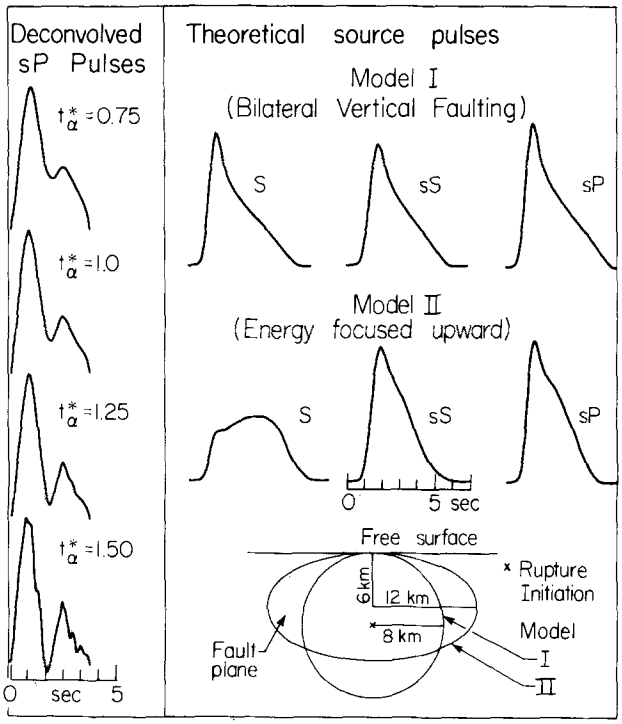

FIG. 4. The figure shows all the source pulses used in computing synthetic S-wave seismograms. Those on the left were deconvolved from the sP phase assuming various values of $t_\alpha{}^*$. Those on the right were computed from the theoretical fault models on the bottom. Either model fits the observed sP pulse, but model II predicts a very different shape for the direct S pulse.

assumed that the Earth's velocity structure has no other significant effect on the seismogram. Inverting this expression gives the source pulse in terms of the deconvolution operation

$$P(t) = F^{-1}[\bar{S}(\omega)/(\bar{I}(\omega) \cdot \bar{A}(\omega, t^*))] \tag{6a}$$

F^{-1} is the inverse Fourier transform and the barred quantities are forward transformed.

Deconvolved sP pulses for a range of assumed values of $t_\alpha{}^*$ from 0.75 to 1.5 are shown on the *left* of Figure 4. The pulses have been windowed out of the deconvolution results using a square window. This method should work reasonably well since the sP phase is by far the largest arrival in the P-wave pulse (see Figure 2). The sharp edges of the square window should cause no difficulty since the S-wave attenuation filter is a strong smoothing operator. The values of the power ratio, r_s,

which were determined by using the deconvolved pulses are plotted as a function of t_β^* in Figure 5 (heavy line). The measured values of the power ratio are shown as horizontal lines. The theoretical curve intersects the observed levels when $t_\beta^* = 5.2 \pm 0.7$ sec.

The results of the preceding calculation would not be valid if the S and sS phases had significantly different spectral content than the sP phase. This type of effect might have been caused by directivity or focusing of energy by the rupture process. Since the takeoff angles of the sS and sP phases differ by only about 10°, their frequency content could not have differed by any great amount. However, it is possible that the direct S phase, which also falls inside the time window W, was much different in frequency content. The range of possible effects of directivity can be determined by examining some theoretical fault models.

Theoretical Fault Models. The fault plane of the Borrego Mountain event is steeply dipping, ($\delta = 81°$) and the observing stations are at roughly right angles to

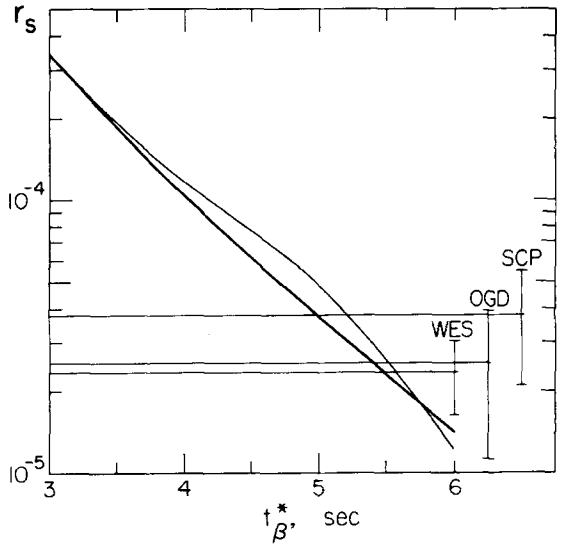

FIG. 5. The figure shows the intersection of the theoretical curves for the S wave power ratio with the observed levels. It appears to occur at a t_β^* value of about 5.2 ± 0.7 sec. The heavy line was computed by using the deconvolved sP pulses and the light by using theoretical fault model I.

the fault plane ($az \sim 110°$). Therefore, horizontal rupture propagation will not cause large differences in the sP, S, and sS phases. The main differences must arise from the vertical rupture propagation. If the fault propagates unilaterally either upward or downward, high frequency energy will be focused in that direction. If the fault propagates bilaterally, the effects of focusing will be negligible. We will begin by considering the bilateral case.

In the fault model proposed for the Borrego Mountain earthquake by Burdick and Mellman (1976), the rupture is presumed to begin at 8 km depth and propagate outward at a constant rate of 2.8 km/sec (0.8 β) to a circular boundary of 8 km radius. This brings it upward to the free surface and downward on the fault plane to 16 km. The displacement distribution is assumed to be the one given by Eshelby (1957), and the dislocation time is presumed to be very small. The model is shown schematically at the bottom right of Figure 4 as model I. The three theoretical S phases are shown at the top of the figure. As expected, there is little difference between them. The theoretical $r_s - t_\beta^*$ curve computed using the theoretical S and sS pulses is nearly the same as for the previous calculation. It is shown in Figure 5

as a light line. This calculation has shown that if faulting was predominantly bilateral in the vertical direction, then the result that $t_\beta{}^*$ is about 5.2 sec is correct. The same would be true if the rupture velocity was very slow or the fault dimension very small.

Fault models which propagate downward to a greater extent than upward generally predict sP phases which are incompatible with the observed arrivals. Also, since the fault appears to have propagated upward to break the surface, this model does not appear to be too reasonable. It is much more likely that if the vertical fracturing was asymmetric, the fault propagated further upward than downward. A model of this type is shown at the *bottom* of Figure 4 as model II. The failure propagates upward 8 km and downward only 4 km so that energy is focused into the upgoing

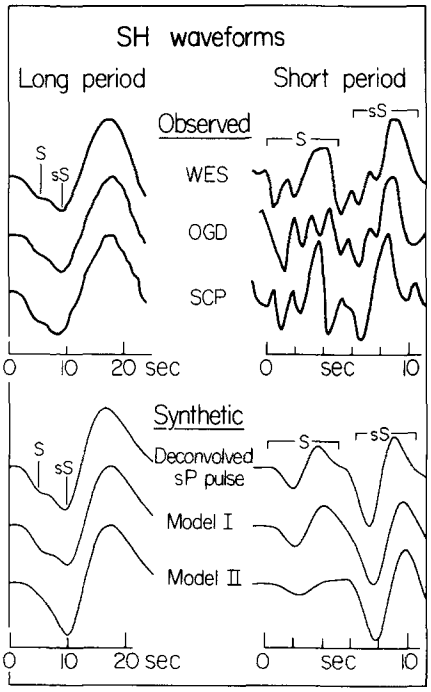

FIG. 6. The figure compares observed long- and short-period SH wave forms to synthetics. The theoretical wave forms computed either by using the deconvolved sP pulse and ignoring directivity or by using model I fit the data. Model II does not fit the observed wave forms.

phases. This can be seen clearly in the theoretical pulses for the model which are also shown in the figure. The theoretical S pulse is much lower in amplitude and longer in duration than the upgoing phases. However, if theoretical wave forms are computed using these pulses, they do not match the data. This is illustrated in Figure 6. The seismograms computed using either the deconvolved sP pulse or the bilateral faulting pulses fit the observed wave form closely. The correspondence between the observed and computed S/sS amplitude ratios is very good for the long periods and within the large uncertainties for the short periods. The seismograms computed using the theoretical pulses for model II do not fit the observed S/sS ratio. The predicted S is too small on both the long- and short-period records. The failure of model II to fit the short-period S waves is very significant. Referring back to the short-period records in Figure 1 one can see that the upward swing of the S and sS phases emerges clearly from the noise in the SCP and WES records. The two phases on the short-period record have approximately the relative proportion predicted by

the bilateral faulting model. If vertical directivity does not have a large effect on the short-period *SH* records, it will not have a measurable effect on the results. To summarize, the preferred value of t_β^* was derived using an effective point source approximation. This method should be acceptable so long as the effects of vertical directivity are negligible. This could occur either because the vertical fracturing was bilateral or because the rupture velocity was low. If vertical directivity was important, it should have affected the short-period *S* records which it did not. Therefore, the value of t_β^* for a travel path between southern California and the northeastern U.S. is roughly 5.2 sec.

t^* for Deep-Focus Events

The short-period *S* waves from deep focus earthquakes generally appear to be much larger than those from shallow earthquakes. The most likely reason for this is that body waves from deep events travel through the highly attenuating upper mantle only once while those from shallow earthquakes go through twice. This implies that t^* is not only a function of distance Δ but of source depth h as well. If most attenuation does occur near the top of the mantle then for $30 < \Delta < 80°$ t^* will be a much stronger function of h than Δ. The attenuation rate of the body waves from some deep South American events has been determined to test the consistency of the observations with current models of the Q distribution.

It is very interesting to compare the t^* values of these deep South American events with the values determined from the Borrego Mountain earthquake because of the source-station geometry for the two events. The body waves for the Borrego Mountain event began at a very shallow depth in the western U.S., penetrated into the lower mantle and emerged in the eastern U.S. The t_β^* for this path appears to be relatively high. This might possibly reflect the fact that the attenuation is more intense on only the source end of the path. It is well known that there is a Richter magnitude difference between the two regions (Booth *et al.*, 1974, Evernden and Clark, 1970) and a number of studies have suggested that this is attributable to a difference in average Q of the upper mantle. (Solomon and Toksöz, 1970; Der *et al.* 1975; Der and McElfresh, 1976, 1978). The body waves from the deep South American events can be used to help resolve the magnitude of this difference. These body waves start downward from a depth of nearly 600 km. This is most probably below any lateral heterogeneity associated with the South American continent or the descending slab (Barazangi *et al.*, 1975). From there, they dive into the lower mantle and make a single passage to the surface either in the eastern U.S. or the western U.S. If the Q distribution along the ray path for the Borrego Mountain body waves is sufficiently asymmetric it may show up as an azimuthal variation in t^* for the body waves of the deep events.

The Data Set. The four seismic events which were selected for study were moderate-sized earthquakes at depths around 600 km. Three of them occurred in Argentina and one of them on the Peru-Brazil border. The locations are given in Table 1. The source pulse from each of the events appeared to be sharp and very simple. The long-period *P* and *S* records both indicate that the source was a single unidirectional spike of short duration. The short-period *P*'s were large and very high frequency, but the short-period *S*'s were moderately sized, simple, and well recorded all across the continental U.S. Some good examples of the long- and short-period *S* waves are shown in Figure 7. It is interesting to compare the amplitudes of the *S* waves in the figure to those of the *S* waves from Borrego Mountain in Figure 1. Even when the difference in gain settings is accounted for the short-period *S*'s from the deep event have much larger amplitudes in relation to the long periods than

those from Borrego Mountain. The effects of the reduction in t_β^* for the deep events are very clear. The recordings selected for study begin at ranges of about 45° and are cut off at a range of 80°. S waves from beyond this distance are very sensitive to the structure of the core-mantle boundary. All U.S. stations in the allowed distance range were examined for record quality. The analysis procedure requires good

TABLE 1

LOCATIONS OF THE DEEP EVENTS

Location	Latitude (S)	Longitude (W)	Date	Time	Depth (km)	Magnitude
Peru-Brazil	9.1	71.3	11/03/65	1:39:3.1	598	6.1
Argentina	27.4	63.3	1/17/67	1:7:54.3	590	5.5
Argentina	22.0	63.5	9/09/67	16:52:01.3	577	5.9
Argentina	27.6	63.2	8/23/68	22:36:51.3	537	5.8

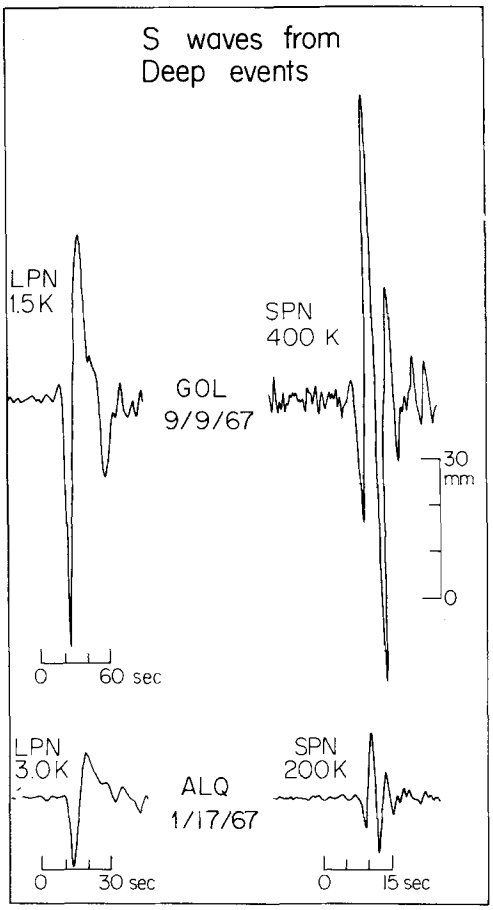

FIG. 7. These are typical short- and long-period S-wave records of deep events. The short-period S is relatively large with respect to the short-period S recorded from shallow events. This is because they have not been as strongly attenuated.

recordings of short- and long-period P and S waves. This drastically reduces the number of acceptable records.

Data Analysis. The value of t_β^* is to be determined from the relative attenuation of P and S waves. The major difficulty with this approach is that the initial frequency content of the P and S pulses is very difficult to determine. Because of directivity, a source may radiate higher or lower frequency S pulses than P pulses

in some directions. It is difficult to model the effect since the fault-plane solutions of the deep events are poorly constrained, and postseismic data are virtually nonexistent. The problem can be circumvented if observations from several different earthquakes are averaged together. There should be no large consistent bias in the frequency content of S with respect to P.

The deep earthquake data can be rapidly analyzed by using the following procedure. A simple measure of the frequency content of both the P and S waves is made for each observation. This is achieved by taking the trace amplitude ratio of the short- and long-period records. Theoretical values of the P and S amplitude ratios are calculated for a family of source models and several different t^* values. The theoretical and observed ratios are compared to find the correct value of t^*. The short period-long period amplitude ratio is defined as

$$R_{S \text{ or } P} = (A_{sp}/A_{lp})_{S \text{ or } P} \tag{7}$$

A is the gain corrected, maximum trace amplitude of either the short-period (sp) or long-period (lp) record. The values of A are measured in the first 10 sec of record after arrival time. As before, all of the source scaling terms are canceled by taking the ratio of the long- and short-period amplitudes. R should depend only on the amount of energy in the short-period frequency band. The amplitude ratio R is very similar to the power ratio r defined by equation (2). r is a more stable measure of the high-frequency signal strength, but R can be much more rapidly determined. When many observations are to be analyzed it is more practical to use the amplitude ratio R.

The observed values of R_S and R_P for the four South American events are given in Table 2. The stations are designated as EUS for eastern U.S. or WUS for western. A comparison of the two groups should indicate whether the western U.S. is much more attenuating then the eastern. We have adopted the map given by Der *et al.* (1975) for determining which stations belong to which group. Several other maps have been published by other authors. Some of these such as the one by Solomon and Toköz (1970) would suggest that stations on the west coast are also on relatively high Q mantle. However, using one of these alternative maps would not strongly alter our conclusions. A separate group of anomalous R determinations is given at the bottom of the table. These measurements will be discussed separately.

Calculated Values of *R*. The family of source models to be used in calculating theoretical values of R is simple but realistic. For this set of fault models, rupture is assumed to start at a point and spread radially at constant speed ($0.8\,\beta$) to a circular boundary (Savage, 1966). Model I in Figure 4 is a representative member of the family. The set of models has two free variables. One of them is the angle between the ray direction and the normal to the fault plane. This value has been fixed at 90° since this is the most probable value. The second model variable is the fault radius. Synthetic P- and S-wave source pulses are computed for a range of values of the source radius. Synthetic short- and long-period seismograms are than computed by convolving in the instrument responses and the Futterman (1962) attenuation operator evaluated at a given value of $t_\beta{}^*$. It is assumed as before that equation (5) holds. R_S and R_P values are determined by processing the synthetic seismograms in the same way as the data. The pulses become longer period as the assumed value of the fault radius is increased, and the values of R_S and R_P decrease. Theoretical curves in the R_S-R_P plane for fixed values of $t_\beta{}^*$ and a range of fault sizes are shown in Figures 8 and 9. The theoretical curves begin in the upper right with the smallest

values of fault radius and drop to lower values of R_S and R_P as fault radius is increased. The complete curve for a set of models drops rapidly downward to lower values of R_S as the value of t_β^* is increased. The data points in Figure 8 are the measured values from eastern U.S. stations. The data points appear to scatter around the curve predicted for the t_β^* value of 3.0. The four symbols represent the

TABLE 2

MEASURED VALUES OF R

Event	WWSSN Station	Δ (deg)	R_P	R_S	Group
11/30/65	GEO	48	0.68	0.0082	EUS
	OGD	50	0.027	0.0073	EUS
	SCP	50	0.072	0.0066	EUS
	WES	51	0.049	0.0096	EUS
	RCD	60	0.19	0.018	EUS
	TUC	56	0.10	0.011	WUS
	ALQ	55	0.090	0.011	WUS
	GSC	62	0.11	0.017	WUS
9/09/67	SHA	63	0.43	0.019	EUS
	GEO	67	0.12	0.011	EUS
	FLO	71	0.125	0.016	EUS
	SCP	69	0.16	0.010	EUS
	WES	70	0.056	0.0065	EUS
	AAM	72	0.10	0.010	EUS
	TUC	75	0.073	0.0052	WUS
	GSC	80	0.073	0.011	WUS
	GOL	78	0.067	0.0044	WUS
8/23/68	ATL	59	0.14	0.0079	EUS
	BLA	61	0.10	0.011	EUS
	OGD	64	0.10	0.0077	EUS
	SCP	64	0.13	0.0085	EUS
	TUC	70	0.088	0.0086	WUS
	ALQ	70	0.059	0.0077	WUS
1/17/67	SCP	69	0.15	0.0093	EUS
	GEO	67	0.14	0.0090	EUS
	FLO	71	0.23	0.017	EUS
	BLA	66	0.21	0.0096	EUS
	ATL	64	0.18	0.0082	EUS
	OGD	69	0.14	0.0075	EUS
	JCT	67	0.22	0.023	EUS
	ALQ	74	0.24	0.013	WUS
	TUC	75	0.26	0.011	WUS
	LUB	71	0.33	0.012	EUS
	GOL	77	0.18	0.0074	WUS
	GSC	80	0.20	0.013	WUS
		Anomalous Measurements			
11/03/65	ATL	44	0.13	0.058	EUS
9/09/67	OXF	67	0.67	0.058	EUS
1/17/67	OXF	66	0.58	0.081	EUS

four different seismic events. It appears that in most cases R_P and R_S measurements from the same event tend to cluster together. This implies that the frequency content of the sources did not change significantly across the eastern U.S. The measured R_P and R_S values for stations in the western U.S. are compared with the theoretical curves in Figure 9. The data points again appear to average around the $t_\beta^* = 3.0$ curve although the scatter is greater. The agreement between the observations from the eastern and western U.S. indicates that the average Q is approxi-

mately the same in the two regions. If correct, this implies that the t^* value determined from the Borrego Mountain observations is a good average value for the North American continent. Figure 10 shows a collection of short-period S wave forms from the two portions of the country for two different events. The records were chosen for the figure only on the basis that they had a good signal-to-noise ratio and that they were radiated by the simplest sources. The figure again shows that the western U.S. observations are not consistently smaller and that they are not consistently different in shape. For comparison, we note that Solomon and

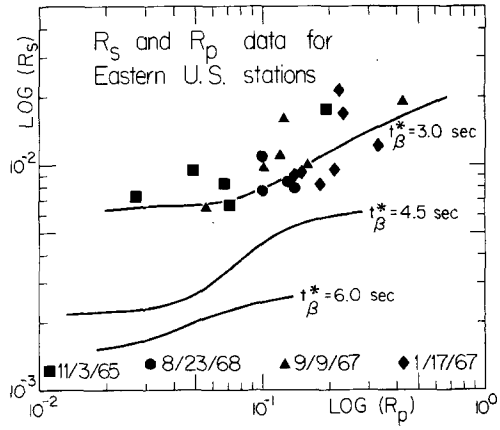

FIG. 8. The curves represent theoretical values of R_p and R_s for a range of fault models. The data points are measured values from the eastern U.S.

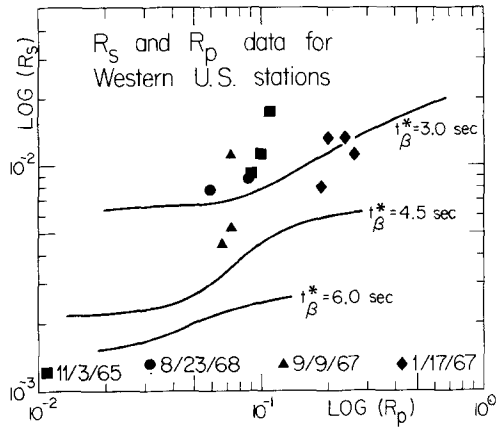

FIG. 9. The curves represent theoretical values of R_p and R_s for a range of fault models. The data points are measured for the western U.S.

Toksöz (1970) found that there should be an average difference of around 2.2 sec in t^* for the two regions, Der and McElfresh (1977) found the average difference for P waves should be about 0.31 sec which converts to about 1.25 sec for S waves. Figures 8, 9 and 10 do not support these results. The three observed values of R which were classified as anomalous all gave very high values of R_S. The short-period S wave form from Atlanta (ATL) for the November 3, 1965 event was very similar to those at the surrounding stations. If it had been attenuated much less than the waves observed at nearby stations, it should have appeared to be shorter period. Also, the ATL record from two other events did not give similarly large values of R_S. Since it is doubtful that Q changed with time, we assume that the station was miscalibrated

for some reason on November 3, 1965. The two large values of R_S of OXF were not caused by large increases in the amplitude of the short-period S but by a drop in the amplitude of the long-period S. This was determined by comparing the absolute amplitude of the ground motion at OXF to several neighboring stations. Since this is the inverse of the behavior caused by an increase in Q, we again feel that these measurements can be excluded from the analysis.

Discussion

Recent advances have shown that it will be necessary to determine the Q structure of the Earth in order to completely determine the velocity structure of the Earth. The work of Randall (1976), Liu *et al.* (1976) and Kanamori and Anderson (1977) has shown that the dispersion associated with attenuation must be accounted for if normal mode data are to be related to body-wave data. This implies that good

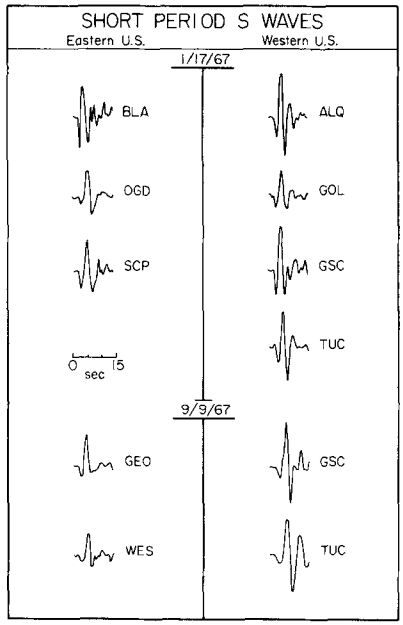

FIG. 10. The figure compares observed short-period S waves from the two portions of the U.S. Each record has been corrected for station gain and normalized by the corresponding long-period record to correct for radiation pattern. The western U.S. records do not appear to be significantly smaller or significantly longer period than the eastern U.S. records.

measurements of the effects of attenuation in any period range have an added significance. The effects of attenuation have been shown to be very large and very easy to observe in the short-period S-wave data. The values of t^* determined from these data should be fairly accurate, and they should supply some reliable constraints on the Q distribution of the Earth. Two recent models of this distribution which satisfy a wide range of observations are model SL1 of Anderson and Hart (1978) and model QBS of Sailor and Dziewonski (1978). t^* is an integral property so it provides little information regarding the detailed structure of the distribution. It should constrain the bulk properties of the model. The t_β^* value for a surface focus event at 35° for SL1 is 3.7 sec. The value for QBS is 4.3 sec. These are significantly lower than the $t_\beta^* = 5.2$ sec value determined for the U.S. The average distance for the deep earthquake observations is about 65°. At this range the SL1 t_β^* value for a 600 km deep event is 3.2 sec. The QBS value is 3.8 sec. The SL1 value is reasonably close to the observed value of about 3 sec, but the QBS value is too high. Taken at

face value, the two observations imply that average Q value of either model for the mantle should be lower overall and that a larger portion of the net body-wave attenuation should occur above 600 km.

Both these results and the result that t_β^* of the eastern U.S. does not differ strongly from that of the western U.S. are dependent on several assumptions we have made. Particularly since this latter result is at odds with some previous work, it is necessary to review what these assumptions were and their possible shortcomings. First, we have assumed throughout this work that the Futterman Q operator adequately describes attenuation in the Earth. This is equivalent to assuming that Q is independent of frequency throughout the seismic band. In the Futterman formalism, Q is allowed to increase with frequency outside the band to preserve causality. If the frequency independence assumption is incorrect, the t^* determinations could be strongly biased. If the Q frequency dependence is itself laterally varying, this could explain why data sets in different frequency bands show different degrees of lateral amplitude variation. It has also been assumed throughout this work that $t_\beta^* \approx 4t_\alpha^*$. The result was derived by assuming that no losses occur in pure compression. However, the result still turns out to be numerically true for the Q model QBS in which finite compressional attenuation does occur. This is because compressional losses do not have a large effect on t_α^* until they become comparable in size to the shear losses along the ray path. The assumption is, therefore, a stable one which has probably not introduced any large errors into the analysis.

The remaining assumptions to be discussed are concerned with the source model chosen for the deep South American events. It does not account for possible azimuthal variation of the frequency content of the source pulse. The actual sources may have radiated pulses with a different predominant period to the eastern U.S. than to the western U.S. This could mask lateral asymmetry in attenuation. It was intended that the choice of four different events from two source regions would average out this type of biasing, but clearly a larger number of events would be desirable. If the sources did all have a strong east-west bias in frequency content, then R_p should have been consistently different for the two regions. Figures 8 and 9 show a great deal of scatter in both R_p and R_s but do not show any such east-west trend in R_p. The high level of scatter is most probably due to either complexity in the source or to variations in the transfer function of the crust at the receiving stations. The vertical scatter in R_s in Figures 8 and 9 may be considered as an indicator of the resolving power of the method. Given the scatter and the small size of the data set it is of interest to pursue the idea that an east-west t_β^* difference of the order of 1.2 sec has been missed (Der and McElfresh, 1976). If this is the case, then the t_β^* value of 5.2 sec from the Borrego Mountain data would be corrected to 4.0 sec. This is the commonly accepted value of t_β^* for surface focus events.

The amplitude measurements of the deep earthquake records were made without regard to predominant period. Some fluctuation in period was observed in the short period S records but not with a consistent regional pattern. Der and McElfresh (1978) reported a bias in S-wave period of about 1 sec. However, they used a much larger data set, and they also used LRSM records. These records can be played at a faster recording speed than the standard WWSSN speed so that time differences of this order are easier to measure.

Conclusions

The Borrego Mountain earthquake body-wave data have permitted a measurement of t_β^* for a ray path from the surface of the southwestern U.S. to the

northeastern U.S. $t_\beta{}^*$ at a distance of about 35° is 5.2 ± 0.7 sec. This value is significantly higher than the commonly accepted one. The deep South American earthquake data allowed a determination of $t_\beta{}^*$ for a ray path beginning beneath the laterally heterogeneous upper mantle, going downward and emerging either in the eastern or western U.S. The $t_\beta{}^*$ value is about 3 sec. This is slightly lower than the value predicted by the recent Q distribution model SL1. The data place some constraint on the bulk properties of the Q distribution which should be taken into account in future Q models.

Acknowledgments

This research was supported by the Advanced Research Projects Agency of the Department of Defense and was monitored by the Air Force Scientific Research under Contract F44620-72-C-0078. The author is grateful for the advice and assistance of Dr. D. V. Helmberger and Rhett Butler which helped considerably in the completion of this work.

References

Anderson, D. L. and R. S. Hart (1978). Attenuation models for the earth, *Phys. Earth and Planet Interiors* (in press).

Anderson, D. L., A. Ben-Menahem, and C. B. Archambeau (1965). Attenuation of seismic energy in the upper mantle, *J. Geophys. Res.* **70,** 1441–1448.

Barazangi, M., W. Pennington, and B. Isacks (1975). Global study of seismic wave attenuation in the upper mantle behind island arcs using pP waves, *J. Geophys. Res.* **80,** 1079–1092.

Booth, D. C., P. D. Marshall, and J. B. Young (1974). Long and short period P-wave amplitudes from earthquakes in the range 0°–114°, *Geophys. J.* **39,** 523–537.

Burdick, L. J. (1977). Broad-band seismic studies of body waves, *Ph.D. Thesis,* California Institute of Technology.

Burdick, L. J. and G. R. Mellman (1976). Inversion of the body waves of the Borrego Mountain earthquake to the source mechanism, *Bull. Seism. Soc. Am.* **66,** 1485–1499.

Carpenter, E. W. (1967). Teleseismic signals calculated for underground, underwater and atmospheric explosions, *Geophys. J.* **32,** 17–32.

Choudhury, M. A. and J. Dorel (1973). Spectral ratio of short period ScP and ScS phases in relation to the attenuation in the mantle beneath the Tasman Sea and the Antarctic Region, *J. Geophys. Res.* **78,** 462–469.

Der, Z. A., P. Masse, and J. P. Gurski (1975). Regional attenuation of short period P and S waves in the United States, *Geophys. J.* **40,** 85–106.

Der, Z. A. and T. W. McElfresh (1976). Short period P-wave attenuation along various paths in North America as determined from P-wave spectra of the Salmon nuclear explosion, *Bull. Seism. Soc. Am.* **66,** 1609–1622.

Der, Z. A. and T. W. McElfresh (1978). The relationship between anelastic attenuation and regional amplitude anomalies of short-period P waves in North America, *Bull. Seism. Soc. Am.* **67,** 1303–1317.

Eshelby, J. D. (1957). The determination of the elastic field of an ellipsoidal inclusion and related problems, *Proc. Roy. Soc. (London), Ser. A* **241,** 376–396.

Evernden, J. F. and D. M. Clark (1970). Study of teleseismic P II-amplitude data, *Phys. Earth Planet Interiors* **4,** 24–31.

Frasier, C. W. and J. J. Filson (1972). A direct measurement of the earth's short-period attenuation along a teleseismic ray path, *J. Geophys. Res.* **77,** 3782–3787.

Futterman, W. I. (1962). Dispersive body waves, *J. Geophys. Res.* **67,** 5279–5291.

Hanks, T. C. and M. Wyss (1972). The use of body-wave spectra in the determination of seismic source parameters, *Bull. Seism. Soc. Am.* **62,** 561–589.

Jordan, T. H. and S. A. Sipkin (1977). Estimation of the attenuation operator for multiple ScS waves, *Geophys. Res. Letters* **4,** 167–170.

Kanamori, H. (1967a). Spectrum of P and PcP in relation to the mantle-core boundary and attenuation in the mantle, *J. Geophys. Res.* **72,** 559–571.

Kanamori, H. (1967b). Spectrum of short-period core phases in relation to the attenuation in the mantle, *J. Geophys. Res.* **72,** 2181–2186.

Kanamori, H. and D. L. Anderson (1977). Importance of physical dispersion in surface-wave and free oscillation problems, *Rev. Geophys. Space Phys.* **15,** 105–112.

Kovach, R. L. and D. L. Anderson (1964). Attenuation of shear waves in the upper and lower mantle, *Bull. Seism. Soc. Am.* **54,** 1855–1864.

Liu, H. P., D. L. Anderson, and H. Kanamori (1976). Velocity dispersion due to anelasticity, *Geophys. J.* **47,** 41–58.

Marshall, P. D., A. Douglas, B. J. Barley, and J. A. Hudson (1975). Short period teleseismic S waves, *Nature* **253,** 181–182.

Mikumo, T. and T. Kurita (1968). Q distribution for long period P waves in the mantle, *J. Phys. Earth* **16,** 11–36.

Randall, M. J. (1976). Attenuative dispersion and the frequency shifts of the earth's free oscillations, *Phys. Earth Planet. Interiors* **12,** 1–4.

Sailor, R. V. and A. M. Dziewonski (1978). Measurements and interpretation of normal mode attenuation, *Geophys. J.* (in press).

Sato, R. and A. F. Espinoza (1967). Dissipation in the earth's mantle and rigidity and viscosity in the earth's core determined from waves multiply relfected from the mantle-core boundary, *Bull. Seism. Soc. Am.* **57,** 829–856.

Savage, J. C. (1966). Radiation from a realistic model of faulting, *Bull. Seism. Soc. Am.* **56,** 577–592.

Solomon, S. C. and M. N. Toksöz (1970). Lateral variation of attenuation of *P* and *S* waves beneath the United States, *Bull. Seism. Soc. Am.* **60,** 819–838.

Teng, T. L. (1968). Attenuation of body waves and the Q structure of the mantle, *J. Geophys. Res.* **73,** 2195–2208.

Yoshida, M. and M. Tsujiura (1975). Spectrum and attenuation of multiply reflected core phases, *J. Phys. Earth* **23,** 31–42.

Seismological Laboratory
California Institute of Technology
Pasadena, California 91125
Contribution No. 2965

Manuscript received November 14, 1977